

6-14-2017

Portable, Powerless Automation of Valve Actuation for Microfluidic Large Scale Integration Technology

Andrew Schmidt

Santa Clara University, aschmidt@scu.edu

Matthew Fitzgerald

Santa Clara University, mfitzgerald@scu.edu

Follow this and additional works at: https://scholarcommons.scu.edu/bioe_senior



Part of the [Biomedical Engineering and Bioengineering Commons](#)

Recommended Citation

Schmidt, Andrew and Fitzgerald, Matthew, "Portable, Powerless Automation of Valve Actuation for Microfluidic Large Scale Integration Technology" (2017). *Bioengineering Senior Theses*. 67.

https://scholarcommons.scu.edu/bioe_senior/67

This Thesis is brought to you for free and open access by the Engineering Senior Theses at Scholar Commons. It has been accepted for inclusion in Bioengineering Senior Theses by an authorized administrator of Scholar Commons. For more information, please contact rsroggin@scu.edu.

SANTA CLARA UNIVERSITY

Department of Bioengineering

I HEREBY RECOMMEND THAT THE THESIS PREPARED
UNDER MY SUPERVISION BY

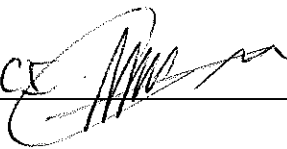
Andrew Schmidt, Matthew Fitzgerald

Entitled

**Portable, Powerless Automation of Valve Actuation for
Microfluidic Large Scale Integration Technology**

BE ACCEPTED IN PARTIAL FULFILLMENT OF THE
REQUIREMENTS FOR THE DEGREE OF

**BACHELOR OF SCIENCE
IN
BIOENGINEERING**

I. EMREARACE 
Thesis Advisor

06/14/17
Date


Department Chair

6/14/17
Date

Portable, Powerless Automation of Valve Actuation for Microfluidic Large Scale Integration Technology

By

Andrew Schmidt, Matthew Fitzgerald

Senior Design Project Report

Submitted to the Department of Bioengineering

of

SANTA CLARA UNIVERSITY

In Partial Fulfillment of the Requirements
for the degree of
Bachelor of Science in Bioengineering

Santa Clara, CA

2017

Abstract

Microfluidic large-scale integration (mLSI) is an emerging field that has the potential to fully automate the biological experimentation and technology development. mLSI offers high-throughput, while maintaining reduced costs and sample size in biochemical tests and experiments. The pneumatic control systems, and the use of solenoid valves that are needed for mLSI make this technology bulky and limits its use to specialized labs. Moreover, since the field is relatively new, few scientists are trained in microfluidic chip design and microfabrication. Eliminating the peripheral equipment from standard testing protocol will allow mLSI to be used in point-of-care settings and more widespread usage of this powerful technology. Our device is a portable, powerless alternative that operates without the use of costly solenoid valves and microcontrollers. In this report, we present a proof of concept demonstrating our device has potential in scalability, high throughput experimentation, and ease of use.

Table of Contents:

Abstract	i
Table of Contents	ii
Table of Figures	iv
Table of Tables	v
Chapter 1: Introduction	1
1.1 Background	1
1.1.1 Valves	2
1.1.2 mLSI	2
1.2 Alternative Strategies	4
1.2.1 Sliding Manifold	4
1.2.2 Magnetic Valve Actuation	5
1.2.3 Thumb Pressure Driven Flow	6
1.2.4 External Power Source Driven Flow	7
1.3 Project Objective	8
Chapter 2: Methods and Materials	9
2.1 Design Description	9
2.2 Technical Drawings and CAD	10
2.3 Device Iterations	11
2.3.1.1 Multilayer Design Description	11
2.3.1.2 Multilayer Design Fabrication	12
2.3.2.1 3D Printed Mold Design Description	14
2.3.2.2 3D Printed Mold Design Fabrication	15
2.3.3.1 3D Printed Mold Design with Pressure Exhaust Description	16
2.3.3.2 3D Printed Mold Design with Pressure Exhaust Fabrication	16
2.3.4.1 Laser Cutter Control Wheel Design Description	16
2.3.4.2 Laser Cutter Control Wheel Design Fabrication	17
2.4 Testing Method	18
2.4.1 General Test Setup	18

2.4.2	Testing Procedure	19
2.4.3	Bright field Microscopy	20
Chapter 3: Results		21
3.1	Multilayer Method	21
3.2	3D Printed Mold Method	22
3.3	3D Printed Mold Method with Pressure Exhaust	23
3.4	Laser Cut Control Wheel Redesign	24
Chapter 4: Discussion		26
4.1	Multilayer Method	26
4.2	3D Printed Mold Design	27
4.3	3D Printed Mold Design with Pressure Exhaust	28
4.4	Laser Cut Control Wheel Redesign	29
4.5	Engineering Standards and Realistic Constraints	30
4.5.1	Economic	30
4.5.2	Health and Safety	30
4.5.3	Sustainability	31
4.5.4	Social	31
4.5.5	Ethical	32
Chapter 5: Future Work and Conclusion		32
5.1	Future Studies	32
5.2	Future Applications	37
5.3	Closing Remarks	38
References		39
Appendix		40

List of Figures

Figure 1.1.1	1
Figure 1.1.1.1	2
Figure 1.2.1.1	3
Figure 1.2.2.1	5
Figure 1.2.3.1	7
Figure 1.2.4.1	7
Figure 2.2.1	10
Figure 2.2.2	10
Figure 2.3.1.1.1	11
Figure 2.3.1.2.1	12
Figure 2.3.1.2.2	13
Figure 2.3.1.2.3	14
Figure 2.3.2.1.1	15
Figure 2.3.2.2.1	15
Figure 2.3.3.1.1	16
Figure 2.3.3.4.1	17
Figure 2.3.3.4.2	18
Figure 2.4.1.1	19
Figure 2.4.1.2	19
Figure 2.4.3.1	20
Figure 3.1.1	21
Figure 3.2.1	22
Figure 3.3.1	23
Figure 3.4.1	25
Figure 4.2.1	28
Figure 5.1.1	33
Figure	40
Figure A.2	41

List of Tables

Table 1.3.1.....9
Table 4.5.1.130
Table 4.5.2.1 31

Chapter 1: Introduction

1.1 Background

Microfluidic Large-Scale Integration (mLSI) is an emerging field that offers low sample volume, while maintaining high-throughput and automation of biochemical experimentation. These benefits can result in tremendous cost reduction and more efficient testing protocol. Since its emergence about 15 year ago, mLSI devices have continued to improve and its range of applications has broadened as a result. However, due to some drawbacks, mLSI has not been used for any paradigm shifting application, “a killer app”, outside of a laboratory setting.

To find meaningful applications outside of a lab setting, technological improvements in standard mLSI are needed. By reducing external equipment and simplifying operation and fabrication, more people will be able to benefit from this robust technology.

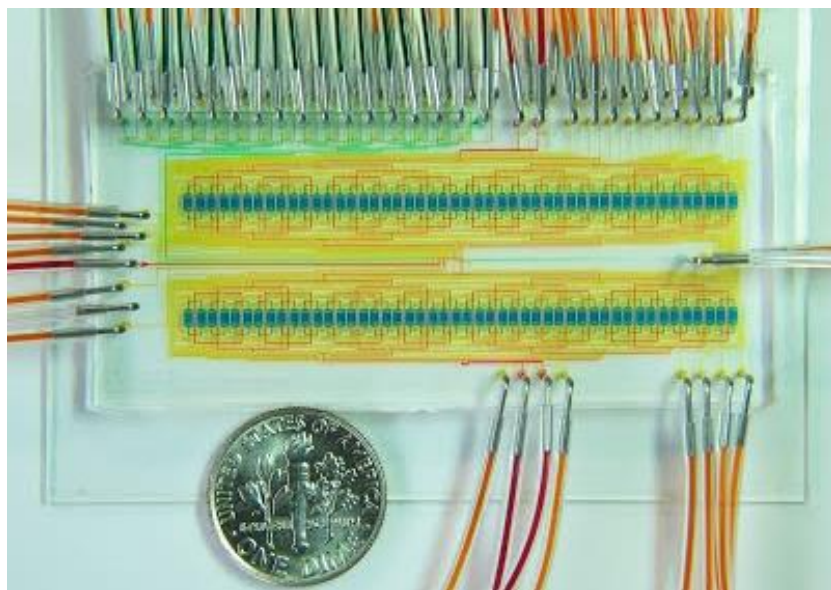


Figure 1.1.1: Standard mLSI chip. The device shown above is a 96-well cell culturing system that operates through a microfluidic platform. ¹

¹ Gómez-Sjöberg, Rafael., et al. "Versatile, Fully Automated, Microfluidic Cell Culture System." ACS Publications. American Chemical Society, 23 Oct. 2007.

1.1.1 Valves

To understand the operation of mLSI devices, an understanding of valves is necessary. mLSI devices operate with constant flow. This means that a pressure is constantly applied, forcing liquid or gas into microfluidic channels. With constant pressure application, there is no way to control the flow of liquids within the device without valves. Techniques such as cell culture, fluidic mixing, and metering all require valves.

Although there are various types of microfluidic valves, we are using push down valves, one of the most common types of valves used in mLSI. Microfluidic devices are generally composed of a flow and a control layer. In a push down valve, the control layer rests on top of the flow layer. By pressurizing the control layer, the thin membrane between the two layers will deflect downwards. This will block the flow of liquids within the control layer, thus closing the valve. A schematic of this process can be seen below in Figure 1.1.1.1.

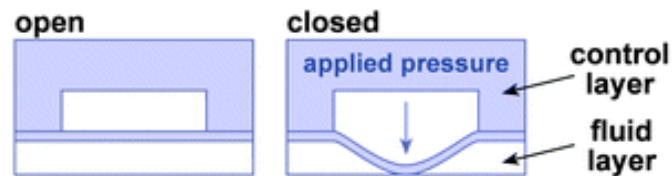


Figure 1.1.1.1: Side view of a push down before and after pressure application. ²

1.1.2 mLSI: Operation and Fabrication

Commonly referred to as “lab on a chip,” because of its miniaturized nature, mLSI has recently been satirically coined “chip in a lab” because of external equipment requirements. Currently, pneumatic control systems and the use of solenoid valves make mLSI technology bulky and limit its use to specialized labs. External software programs, such as Arduino and LabVIEW, are often required to automate experiments.

² Perry et al.. "Design Rules For Pumping And Metering Of Highly Viscous Fluids In Microfluidics." LoC 2010.

Fabrication of mLSI chips begins with photolithography. Substrates must be prepared with the necessary features for mold fabrication. This process requires specialized equipment and a clean room, including spin coaters, hot plates, and mask-aligners. Soft-lithography is used for the actual mLSI chip fabrication. This process also requires a clean room and external equipment, such as centrifuges, plasma cleaners, and microscopes for alignment of multi-layer devices. The microfabrication process requires basic photolithography and soft-lithography skills. The materials used throughout these processes are relatively inexpensive. Proper use of the equipment is essential for successful mLSI experimentation and therefore requires training.

Since this field is relatively new, few engineers and scientists are trained in the area. As a result, labs not specialized in microfluidics often need to outsource any microfluidic testing they wish to complete. Pneumatic control systems, and the use of solenoid valves are some peripheral components needed in mLSI and they add to the cost and complexity of the mLSI device testing. Eliminating these components, or simplifying their operation, from standard mLSI protocol can allow for a larger number of individuals to benefit from microfluidic technology.

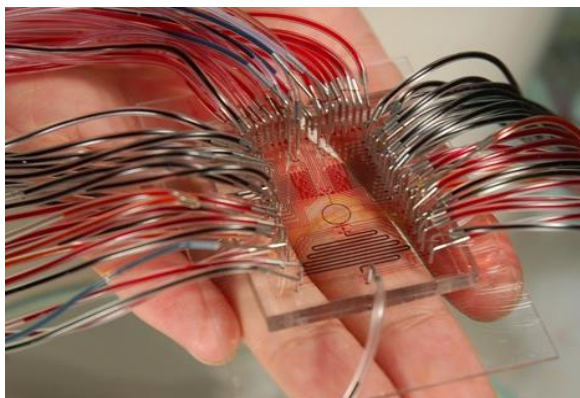


Figure 1.2.1.1: Example mLSI chip used to perform 1,024 parallel chemical reactions. Each of the input wires required operation via an external valve source controlled by computer program and user who wrote the program.³

³ Wang, YJ, et al. "An Integrated Microfluidic Device For Large-Scale In Situ Click Chemistry Screening." Lab On A Chip. 16 Sept. 2009.

1.2 Alternative Strategies to Improve mLSI

Many research groups are working on methods to improve the portability of mLSI devices, as well as simplify their operation for applications outside of traditional lab settings. There have been many clever attempts and our team looks to draw from their success, but none of the current strategies have been widely adopted.

1.2.1 Sliding Manifold

In one recent study, A-line Inc. demonstrated instrument-free pneumatic actuation using sliding manifolds.⁴ These manifolds are inspired from the Jacquard-style mechanism used in the textile industry for weaving patterns, such as brocades into fabric, and include two main components: (i) a control plate with pilot lines used to supply pressure to the device, and (ii) a program plate with an array of features used to program the sequence of pressure states to be delivered to the device. The two plates are assembled using a lubricant and their relative position is used to control the sequence of operations. The overlap between features in the top and bottom plate determines the state delivered to the device. Examples of these manifolds and their use to control on-board valves is shown in Figure 1.2.1.1. These sliding manifolds are limited geometrically. The only opportunity for scale without a complete redesign is to make the device much larger, which defeats much of the purpose for developing an mLSI alternative.

⁴ Begolo, Stefano. "Instrument Free Control of Microfluidics." *ALine, Inc. - Accelerated Microfluidic Development*. MicroTAS, 11 Oct. 2016.

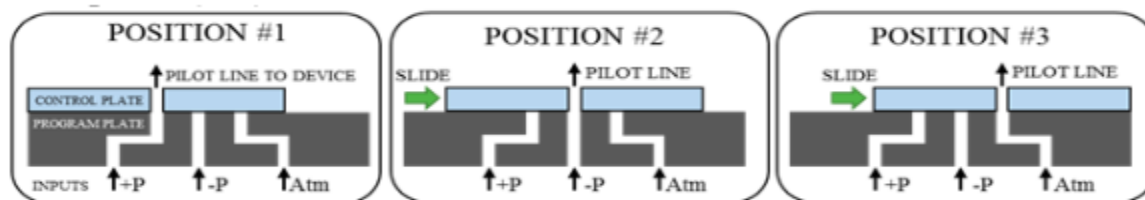


Figure 1.2.1.1. Principle of operation of a sliding manifold with a pilot line and three positions to deliver different actuation states.⁵

1.2.2 Magnetic Valve Actuation

Another recent study made use of PMMA (Poly-methyl-methacrylate) for the body of the device and magnetic actuators for mixing.⁶ The system is a frugal alternative to traditional mLSI technology. In this design, two magnets about a millimeter in size were used to open and close a single valve. To scale up this device, many magnets would be required to actuate valves, and the magnet size will have to be reduced as well. The external magnets were 12 mm x 15 mm, and the internal magnets were 6.35 mm x 0.8 mm. Microfluidic channels are often fabricated in the micron range. As channels increase in size, scalability becomes tough and a device loses the benefits of low sample sizes and high throughput experimentation. The actuation of the magnetic valve is shown in Figure 1.2.2.1.

⁵ Du, Wenbin., et al. "SlipChip." Lab on a Chip. The Royal Society of Chemistry, 15 May 2009

⁶ Harper, Jason C., et al. "Magnetic-adhesive Based Valves for Microfluidic Devices Used in Low-resource Settings." *Lab on a Chip*. The Royal Society of Chemistry, 28 Sept. 2016.

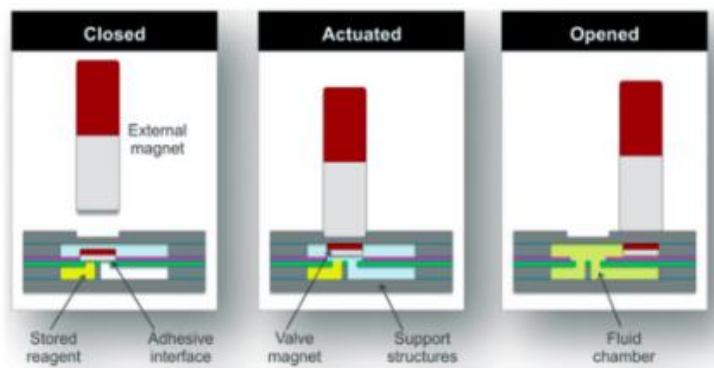


Figure 1.2.2.1. General setup of the magnet manipulated chip. Movement of the two magnets allows the separated liquids to diffuse into one another, evident by the change in color.

1.2.3 Thumb Driven Pressure Flow

Thumb and finger driven pressure flow has also recently been explored as another method to reduce the amount of peripheral equipment and simplify the operation of microfluidic devices. This method is a promising frugal alternative to current industry standards. One such study actuated two valves using only thumb pressure in a proof of concept test.⁷ The thumb pressure opened reservoirs filled with colored liquids and allowed them to mix, with a colorimetric change indicating successful valve actuation. The thumb-driven functionality of the device is demonstrated in Figure 1.2.3.1. By using check valves that only open when pressure is applied, various preloaded reagents can mix, eliminating the need for a constant pressure source. A major drawback is that quantifying thumb pressure is difficult, which limits accuracy and possible applications. Scaling up for actuation of multiple valve combinations is also difficult as thumbs are far larger than the average pressure inlet.

⁷ Wentao, Li., et al. "Squeeze-chip: A Finger-controlled Microfluidic Flow Network Device and Its Application to Biochemical Assays." Lab on a Chip. 23 Feb. 2012.

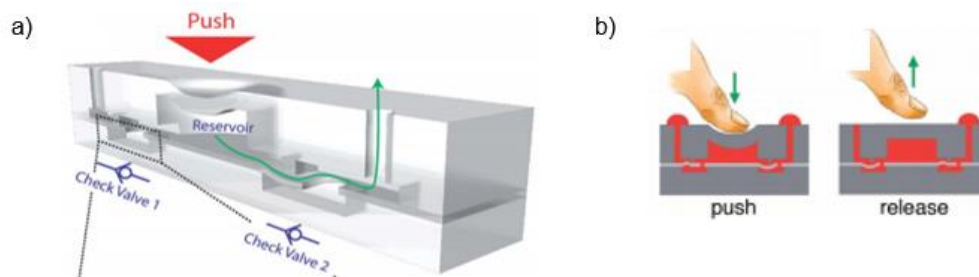


Figure 1.2.3.1: a) General structure of thumb driven chip valve. It was designed with two check-valves and a reservoir in between. b) Visual representation of thumb pressure application to the channels.

1.2.4 External Power Source Driven Flow

Another study we looked to draw from details a completely autonomous microfluidic system that uses a micro-fuel cell to both power the chip and drive fluid flow.⁸ This proof-of-concept experiment demonstrated fluidic flow rate can be controlled by energy input from a fuel cell. Fluid was driven from one reservoir to another to demonstrate this functionality. We are attempting to drive fluid flow without an external power source as they require regular replacement. A general schematic of the device is shown in Figure 1.2.4.1.

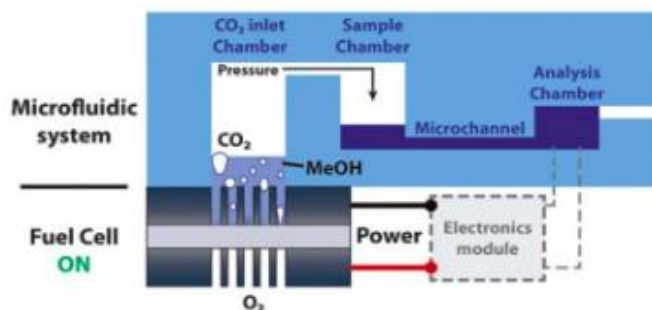


Figure 1.2.4.1: General setup of the fuel cell powered chip. Pressure from the CO₂ drives the flow of fluid in a microchannel, while the fuel cell generates power itself.

⁸ Esquivel, Juan Pablo, et al. "Fuel Cell-powered Microfluidic Platform for Lab-on-a-chip Applications." *Lab on a Chip*. The Royal Society of Chemistry, 10 Nov. 2011.

1.3 Project Objectives

The overall goal of our project is to provide a novel alternative to current mLSI devices that will allow for the widespread use of microfluidic technologies throughout rural clinics. Our system aims to eliminate traditional mLSI equipment that limits the technology use to trained experts. By creating an easy-to-use, robust alternative to current industry standards, the availability of this technology will increase substantially. Simply put, we hope to reduce the difficulty of operating microfluidic systems, while also maintaining the high throughput nature and automation capabilities that microfluidics allows for.

To confirm these aspects, our project can be broken down into two phases. Our first phase will be to demonstrate we can create a device that may open and close valves in a powerless and robust manner. The second phase will be dedicated solely for optimization of the device. Since this field is still being explored, this project aims to create an entirely new device. The emphasis is to create a device that solves portability and operation problems related to mLSI, rather than aiming to solve a specific clinical application. Once we have an operational and optimized device, we hope it can be applied to a variety of clinical applications. To reach this goal we set up distinct milestones, by quarter, as laid out in Table 1.3.1 below.

1.3.1 Table 2: Project Milestones Timeline

Quarter	Goals
Fall	<ul style="list-style-type: none">• Review Alternative Strategies• Fabricate initial prototype• Develop budget• Obtain funding
Winter	<ul style="list-style-type: none">• Demonstrate proof of concept test• Prepare for Presentation at Biomedical Western Regional Conference hosted by BYU
Spring	<ul style="list-style-type: none">• Optimize device• Prepare for Senior Design Presentation

Chapter 2: Material and Methods

2.1 Design Description

Our design looks to draw from and improve upon previous attempts at minimizing external equipment and maximizing ease of use. Our device is powerless, and offers improved potential for scalability and accuracy. Our chip contains a rotating array of channels that connect to an array of outer channels. By rotating the inner array, we can open and close valves with a single pressure input. These inner and outer channel arrays can be easily modified to comply with a wide variety of experimental protocols. Figures 2.2.1 and 2.2.2 in section 2.2 provide a visual representation of the functional operation of our device.

2.2 Drawings and CAD

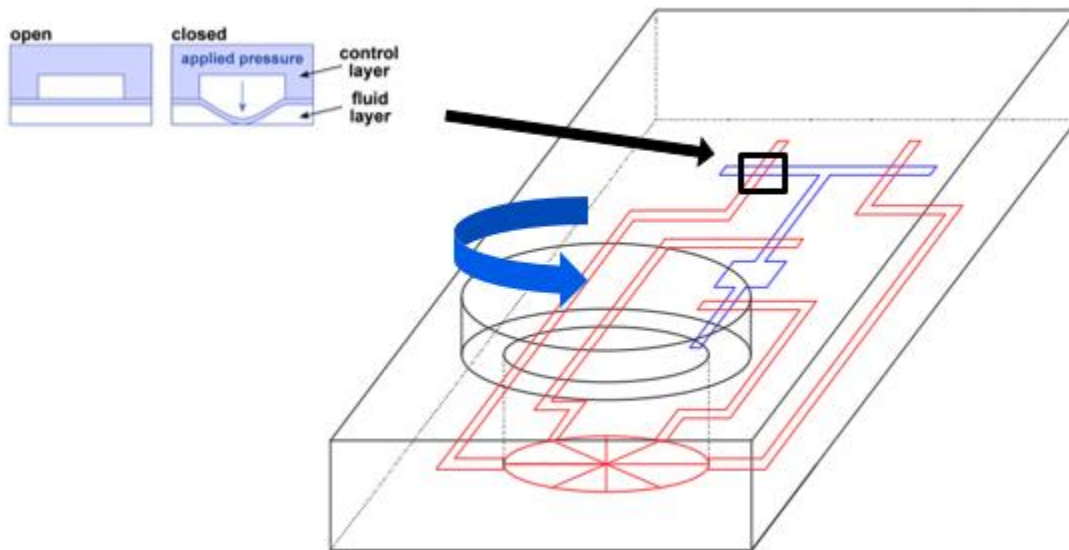


Figure 2.2.1: Simplified technical drawing of our device. Highlighted is the push down valve interface between the red control channel and blue flow channel.

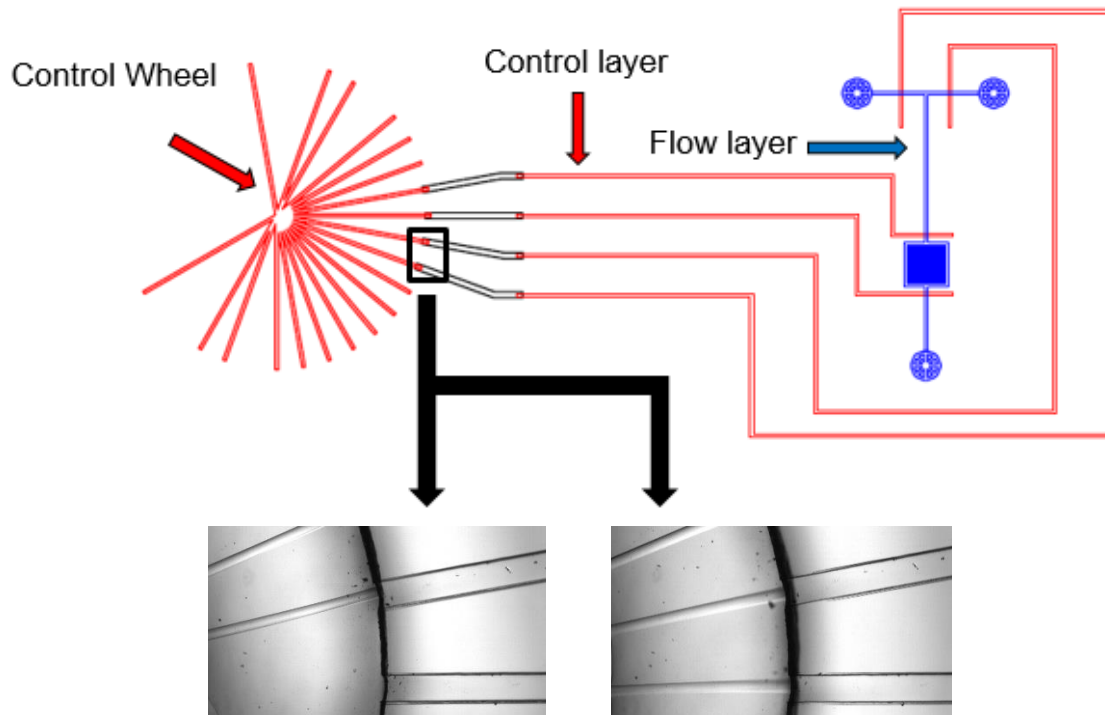


Figure 2.2.2: Top view of our device. Highlighted is the interface between the inner and outer control channels.

2.3 Device Iterations

Over the course of our project, we had several different device iterations. Each iteration offered new information and data that lead to the optimization of the device. All new knowledge led to distinct changes that were made in the following iteration. Also noteworthy is that each iteration was slightly modified various times, and described in this report are the main designs and their significant takeaways.

2.3.1.1 Multilayer Design Description

The first design consisted solely of three PDMS layers. The goal of this initial design was to determine whether we could translate pressure from the inner channel array into the outer control channel array. The multiple-layer aspect of the chip was to ensure proper sealing and prevent pressure. The sealing between the dynamic, circular control wheel and the main chip body was later learned to be one of the most important aspects of the device, as without a proper seal the pressure supply would practically be entirely lost to leakage. While the sealing between layers was optimal in this design, manipulating the device in order to control fluids would be very difficult to achieve. Although an application would be hard to achieve with this device, we were able to successfully demonstrate the dynamic control of two control lines.

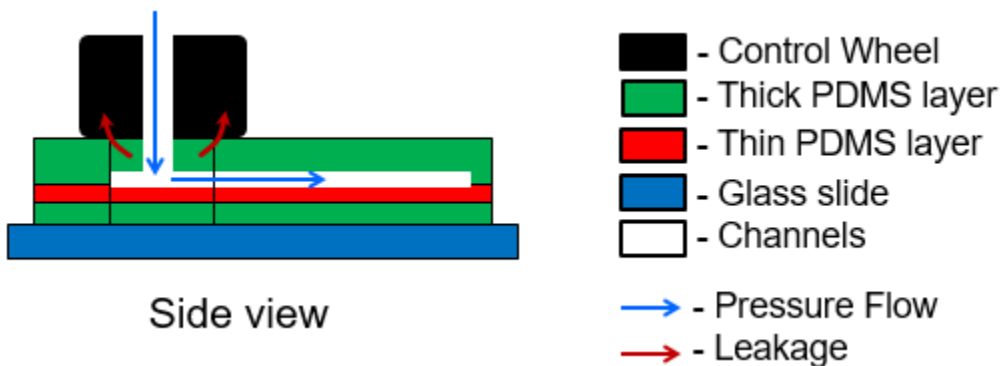


Figure 2.3.1.1.1: A side view schematic of the device produced using photolithography is shown above. The varying colors represent the different layers and components of the device, detailing the complexity of this iteration.

2.3.1.2 Multilayer Design Fabrication

Standard photolithography procedures were used to fabricate a silicon wafer mold. SU-8 2035 photoresist was spun at 1000 rpm for one minute onto a silicon wafer to produce features that were 100 μm in depth. The photoresist layer was then patterned with our AutoCAD design using UV exposure. The channels were developed for about five minutes using SU-8 developer. Channels varied from 50 μm – 500 μm in width in order to test the effectiveness of various channel widths.

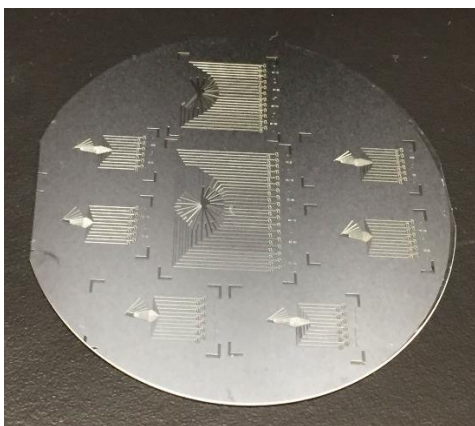


Figure 2.3.1.2.1 8 designs varying in channel width and spacing between the channels. Displayed here on a silicon wafer after the photolithography process. (probably need better image)

Soft lithography was used to fabricate the chips themselves. The top layer was made using PDMS in a 1:10 ratio and was patterned with the channels and features using our silicon wafer mold. Before pouring this PDMS layer onto the silicon wafer, the mold was treated with Trimethylchlorosilane (TMCS), an anti-adhering chemical surfactant. The middle thin layer was made using PDMS in a 1:20 ratio and the bottom layer was made using PDMS in 1:10 layer. The top and bottom layers were partially cured for 35 minutes and the middle thin layer was cured for 20 minutes at 80° C, after which point all three layer were laid on top of one another and placed back in the oven for two hours to complete the thermal curing and bonding process.

The central channel array was punched using a 1 cm biopsy punch. Several different methods of cutting motion were experimented with to minimize the deformation of the punch, some being much more successful than others. After experimenting with the

different punching methods, we determined that a slow, single direction, rotating punch provided us with the most consistent surface, which would allow for the best seal between the two boundaries.

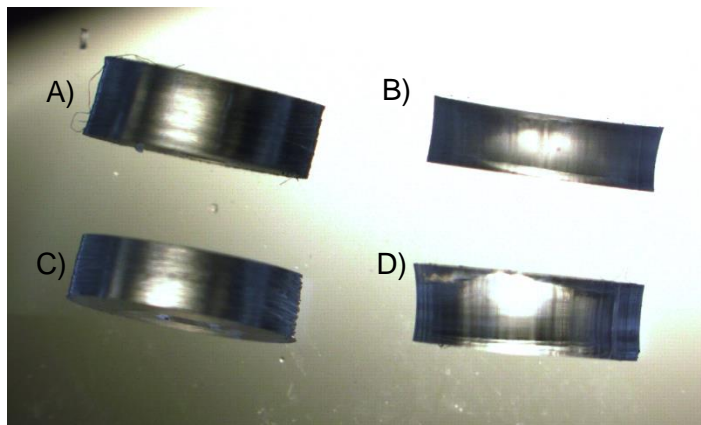


Figure 2.3.1.2.2: The image above shows four different punches created using four separate techniques. (A) Represents a slow single direction, turning punch. (B) Represents a fast, vertical, no rotation punch. (C) Represents a multiple direction, turning punch (D) Represents a slow, vertical, no rotation punch.

The fully cured chip was then punched with pressure exhaust holes on the main body of the chip and a single pressure inlet was punched in the control wheel using the Schmidt Press punch device. An acrylic handle was cut at the SCU Maker Lab using the Epilog laser cutter. The handle and central channel array were bonded together using EA E-30CL Locite Brand epoxy.

The fully cured chip, minus the control wheel, was then bonded to a glass slide using 30 seconds of oxygen plasma treatment on the bottom face of the chip and top face of the glass slide. A fully fabricated device can be seen below in figure 2.3.1.2.3.

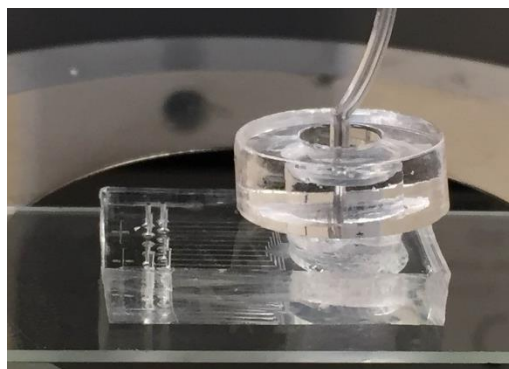


Figure 2.3.1.2.3 A completed version PDMS chip bonded to a glass slide. Includes tube for pressure input and laser cut handle bonded to the chip itself.

2.3.2.1 3D Printed Mold Design Description

Although we were able to optimize the seal between the control wheel and the main chip, there were still several issues with the standard fabrication protocol that did not allow for the optimal performance of the device. These issues with performance forced us to pursue another mode of fabrication.

To optimize the seal between the control wheel and the main chip, we abandoned the biopsy punching method in favor of a 3D printed mold. We designed a mold that eliminated the need for punching the chip simply by using strategic obstruction. Two separate molds were made, one that would serve as the mold for the main chip body and the other that would be used for the control wheel. The designs, including the positive control channels, were designed using SolidWorks and then outsourced to Shapeways to be 3D printed. Shapeways is a third-party, 3D printing service company that has the capability of printing objects with a resolution that makes them suitable for microfluidics. 3D printers at Santa Clara were explored but determined to not have high enough resolution for our microfluidic features.

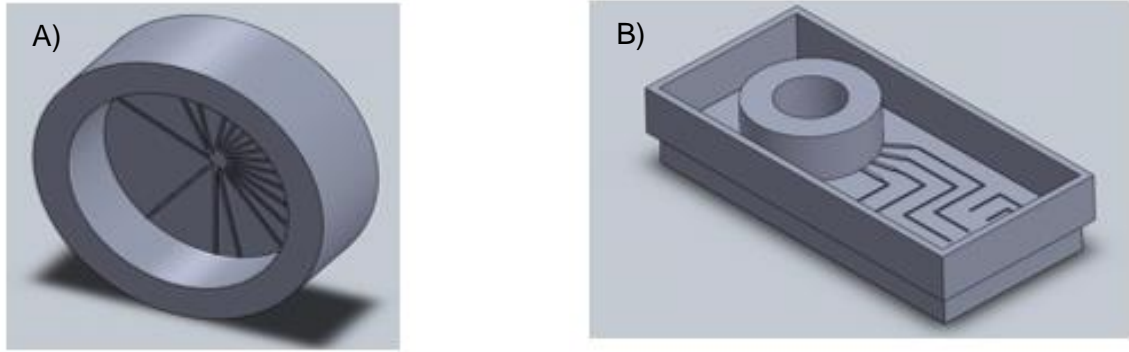


Figure 2.3.2.1.1: The images represent the SolidWorks rendering of the 3D molds. (A) shows the mold that was used to produce the control wheel, while (B) was the mold used for the remainder of the main chip body.

2.3.2.2 3D Printed Mold Design Fabrication

The molds were treated TMCS, 1:10 PDMS was poured into them, and then the molds were placed in an 80° C oven to thermally cure. Upon removal, the chip was punched with pressure exhaust holes, a pressure inlet, and bonded to a glass slide using the punching and oxygen plasma treatment methods described previously.

Through several trial and error experiments, we determined that in order for the control wheel channels to maintain their binary nature, a thin, sealing layer of PDMS was applied to the bottom of the control wheel. This thin PDMS layer would then only allow for air to escape into a channel when both the inner and outer channels were aligned properly.

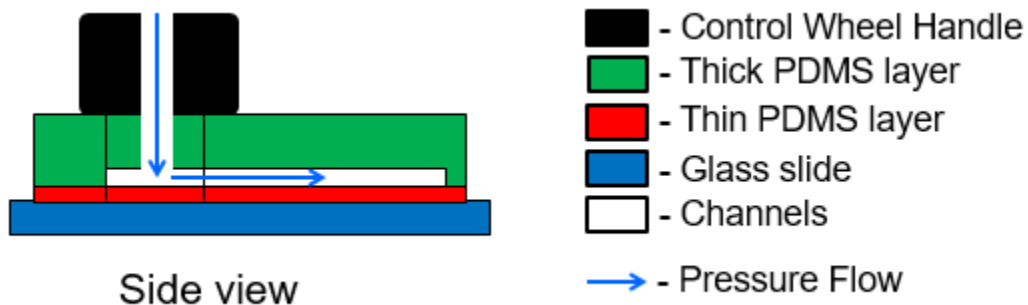


Figure 2.3.2.2.1: The side view schematic above represents the next generation of our device that was fabricated using 3D printed molds. The red section of the chip represents the thin PDMS layer that is used for sealing.

2.3.3.1 3D Printed Mold Design with Pressure Exhaust Description

The results gathered using the 3D printed mold method revealed that a high-pressure pocket beneath the control wheel caused irregularities in our pressure readings. Because of the uniformity of the 3D printed molds, pressurized air that previously escaped upward between the interface of the control wheel and the main chip body was now building up underneath the control wheel. This caused all channels to pressurize rather than the desired channels, and caused the control wheel to pop out of the main chip. As a result, a pressure exhaust was implemented.

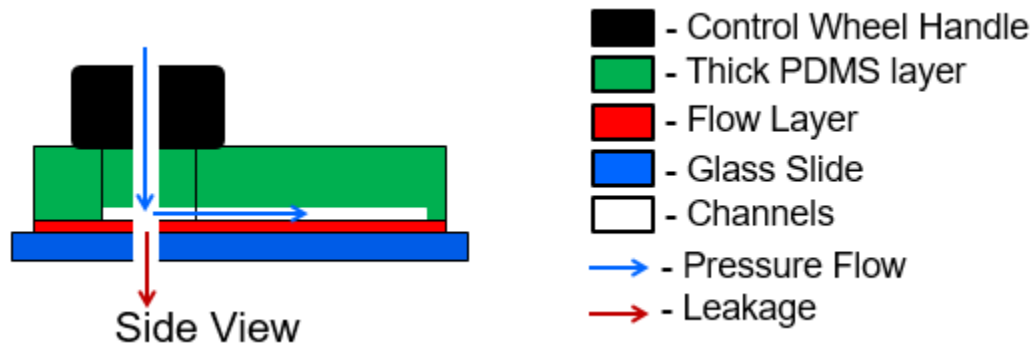


Figure 2.3.3.1.1: The image represents the exhaust port generation of our microfluidic device. The arrangement was completed using a glass slide, which then became a piece of acrylic.

2.3.3.2 3D Printed Mold Design with Pressure Exhaust Fabrication

The fabrication of this iteration was essentially the same as the 3D printed mold design. A glass scorer was used to create a small pressure exhaust in a glass slide beneath the control wheel.

2.3.4.1 Laser Cutter Control Wheel Design Description

At this point in our project, two major issues had to be addressed. The pressure exhaust fixed the issues associated with the high-pressure pocket underneath the control wheel, but reduced output pressure to the point where valve closure would have been quite difficult. Also, as this device is intended to be used as a POC device in rural locations, it should be operated without the need for a microscope. All iterations to this point had to be operated with a microscope for visual confirmation of proper channel alignment.

The main objective of this design was to focus on the alignment of inner and outer channels without having to use a microscope, as well as incorporate a redesigned pressure escape. This current generation of our microfluidic device was fabricated in a rather unorthodox manner for the field of microfluidics. Acrylic was chosen as the new material for the control wheel for its transparent properties and rigidity that aids the ability to rotate the control wheel. A heptagonal and trench design were proposed as their geometric properties would allow a user to feel a change in state upon control wheel rotation and ensure perfect channel alignment.

Also, the pressure exhaust was redesigned so that the input pressurized air would not escape directly through the bottom of the control wheel. Instead, excess air that flowed through the control wheel channels escaped through the bottom underneath the punch. This ensured that enough pressure would be conserved within the chip to close valves, while not too much would build up underneath the chip.

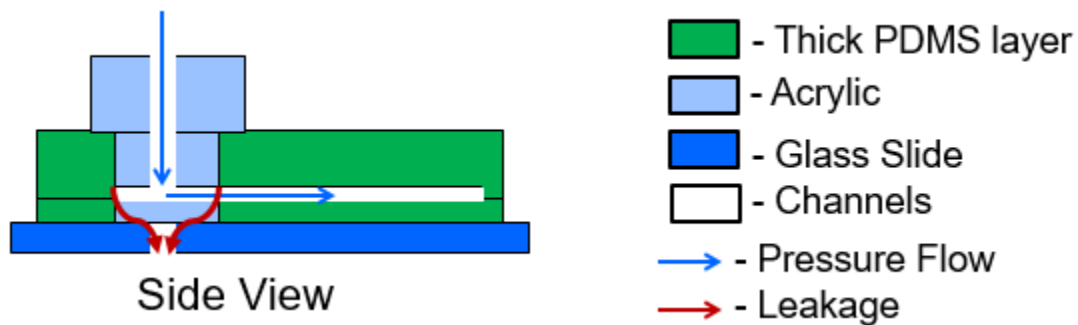


Figure 2.3.3.4.1: Side view schematic of the final chip design using acrylic control wheels.

2.3.4.2 Laser Cutter Control Wheel Design Fabrication

Using AutoCAD, both the heptagonal and trench design channel arrays were created. Then using the Epilog Laser Cutter in the Santa Clara University Maker Lab, the channels were rastered using three passes with the Laser Cutter at low power. Then the acrylic pieces were cut out using the laser cutter at higher power, as well as their respective handles. The two pieces were bonded by applying a small amount of acetone between the pieces and let set for a 24-hour period.

In order to make the main chip body, a replica of the inner piece was created and connected to a glass slide using epoxy to create a channel-less outer chip mold. Standard soft-lithography protocol was used to create the outer chip using 1:10 PDMS.

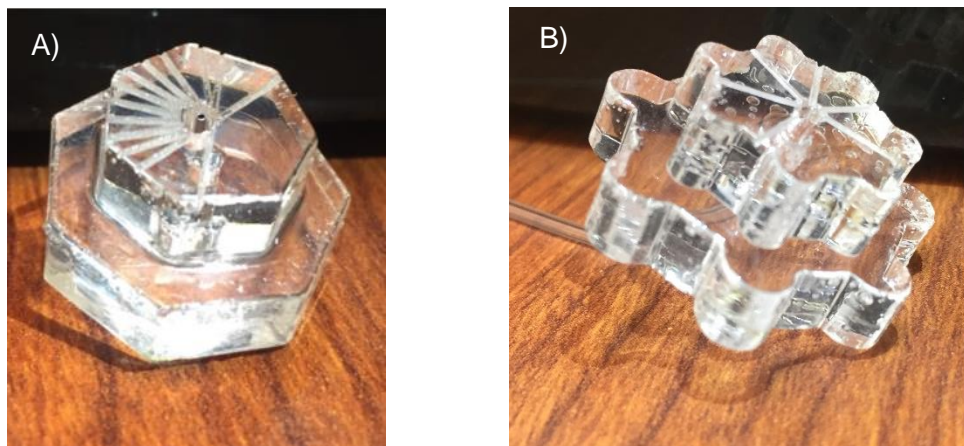


Figure 2.3.4.2.1: A) Heptagonal design B) Trench design. Both acrylic pieces were cut and engraved using the Epilog Laser Cutter.

2.4 Testing Method

Most the experimentation done was attempted to gauge and compare pressure inputs and outputs. To optimize the functionality of our device we needed to quantify the pressure entering our chip through the control wheel, and the resulting pressure in the external channels of the main chip body. In order to do so, we combined algorithm development with circuitry hardware and finally paired these two with our microfluidic control system. The pressure readouts have allowed our team to monitor the crosstalk between channels, as well as the pressure leakage our device experiences.

2.4.1 General Test Setup

Our testing method was constructed and derived mainly from current standards used for microfluidic testing. The general testing method used for most iterations involved using an Arduino board and sequence of code to convert voltage measurements into pressure read-outs. Our pressure sensors were purchased from a third-party supplier. The sensors were integrated chips, or ICs, that were mounted onto the breadboard that contained the rest of our circuit schematic. The sensors measure an input pressure, and

convert it to a respective voltage. The breadboard was built with a circuit to measure the output voltage from the pressure sensors. This output voltage was then read and recorded by our Arduino code. The data collected from the Arduino program was then imported to Microsoft Excel, where we took the voltage readouts and converted them back into pressure readings.

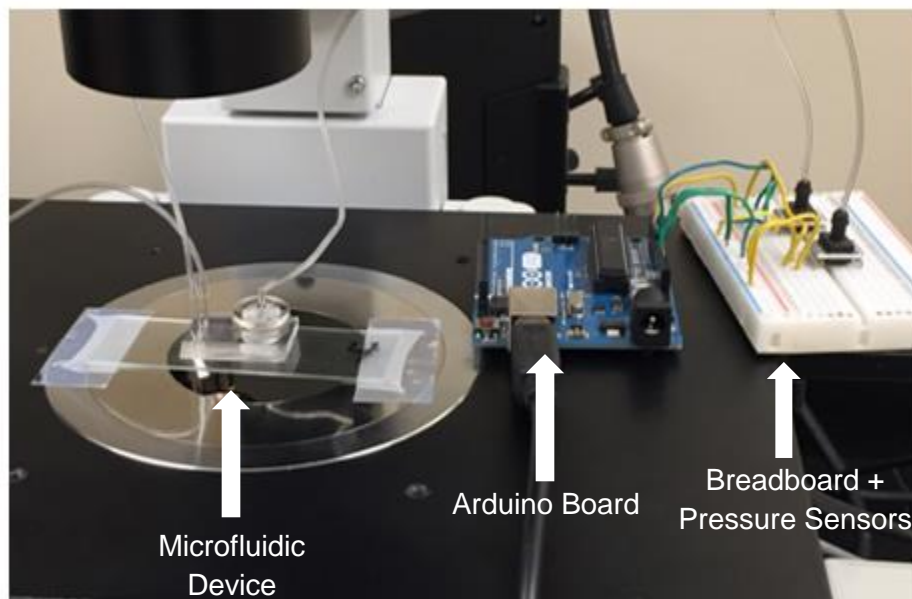


Figure 2.4.1.1: The schematic and test setup represented above show, in full detail, the components of our microfluidic chip and the multi-component testing system.



Figure 2.4.1.2: Direct view of chip setup. Highlighted is the pressure inlet, handle, chip, and glass substrate.

2.4.1 Testing Procedure

The following is the general testing method for our various device iterations. A single pressure input was inserted into the control wheel. Two output pins extending from the

pressure sensors were connected to the outer channels of the main chip. Pressure was applied via an external air compressor to the chip. The control wheel was rotated in various directions to determine the resulting pressure in the outer channels. By continuously monitoring the resulting output pressures, we were able to characterize the crosstalk between the channels in various configurations, as well as determine the extent of pressure leakage from the chip.

2.4.3 Bright-field Microscopy

Until our final prototype design, aligning the inner and outer channel arrays was one of the most difficult aspects of the operation of our device. It is evident through analyzing our data, that over-correcting for misaligned channels causes issues with the functionality of the device. Since we are attempting to create a system with a high-degree of control, we cannot afford to allow for these inconsistencies in pressure application. In order to facilitate the alignment process without actually making physical alterations to the device, an imaging system was needed. We were supplied with a bright-field microscope by our advisor's research lab to use for the alignment of our channels. The microscopy was also used for troubleshooting errors in our device. Some crucial design flaws were unveiled through image analysis, like the ones below. The large, dark portion in the center of the image shows a gap created from irregularities in the diameter of our punch. This issue was discovered and resolved because of our bright-field microscopy techniques.

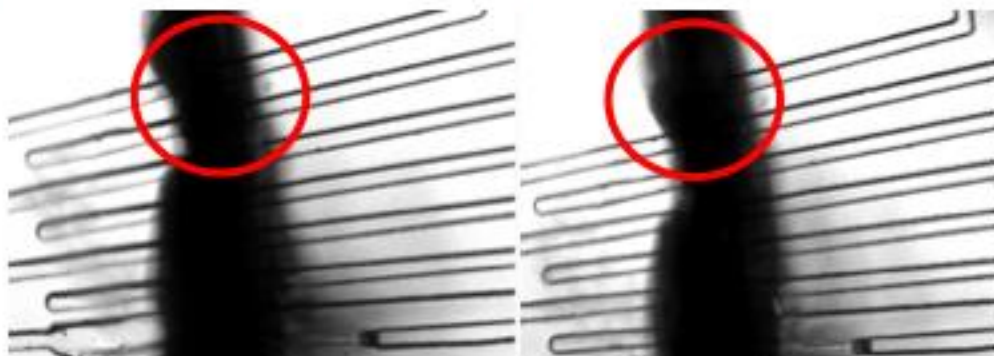


Figure 2.4.3.1: The figure above represents two bit-states of our device during operation. The images taken to allow for this alignment were done so with an Olympus Bright-Field microscope supplied by the SCU School of Engineering.

Chapter 3: Results

Through several iterations we were able to continuously alter our system to both provide a proof of concept and then begin to optimize the fabrication and operation of our device. The alterations were made based on our interpretation of the pressure readings that we recorded, through several trials, with each iteration. With each phase, we took away key insights which we used to improve the necessary components about what needed to be improved and which of the components needed to be altered to facilitate this.

3.1 Multilayer Method

The data we collected from our initial design provided our first proof of concept. The pressure differential between connected and disconnected channels was significant. We successfully demonstrated the ability to switch between states of high or low-pressure application. Additionally, cross talk between channels was reduced to near zero, which ensures that the pressure being applied is only being done so to the desired channels. The following figure represents the demonstration of the dynamic nature of our device.

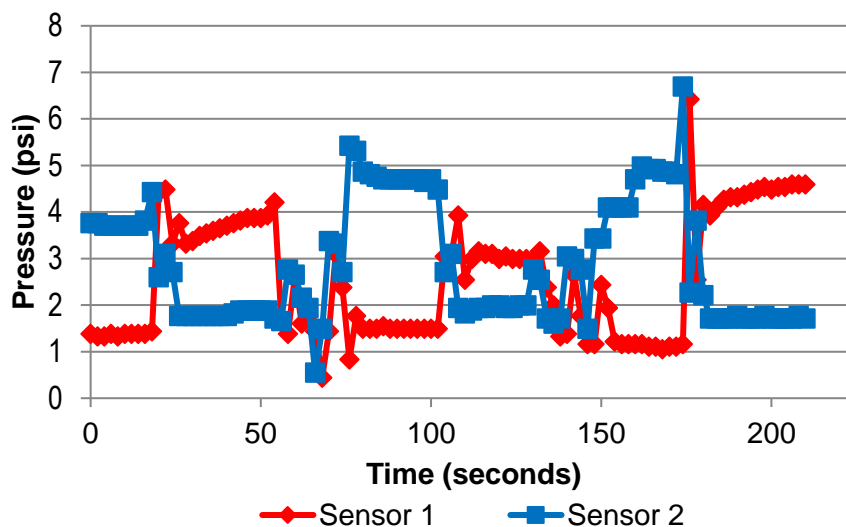


Figure 3.1.1: The figure above represents the continuous pressure output values that were achieved with the first iteration device. The two sensors were connected to adjacent channels and then used to produce readouts that indicated pressure values. The higher-pressure values represent that closed-valve state, while the lower values correspond to an open valve. Pressure input was 10 psi.

Following the successful operation of this device, a few keynote pieces of information were taken away. We learned generating a strong pressure differential with a dynamic component present in the system was possible. Along with this, we learned that because there was near zero cross talk, the sealing between two PDMS layers was strong enough to withstand the on-chip pressure application. Although these notable aspects of this design were very positive, there were also a few takeaways that needed to be improved upon in order for the device to make a real-world impact. One of these was the fabrication method of the device. Complete production of this system took significant time, precision, and materials. Multiple layers of PDMS, all of which were different ratios of the two-part polymer mix, meant that several batches of the polymer needed to be prepared and made for a lot of room for error. Since the entirety of the PDMS prepared can be used, this process can be very wasteful. Finally, the complexity of the fabrication would cause for difficulty, as well as elongated training time, for scientists who wish to prepare these devices in the future. All of this information was taken into consideration for the next iteration of our microfluidic system.

3.2 3D Printed Mold Method

Data collected from the 3D printed mold method was not nearly as strong as the data that was obtained from the initial, multilayer method. The molds reduced the complexity and length of the fabrication process significantly, but had significant surface roughness, which was the cause for many of the problems with this fabrication technique. A positive takeaway from this iteration was that the 3D printed method produced a uniform interface between the control wheel and the main chip body. Due to this change in fabrication, there was nearly no pressure leakage compared to the previous iteration. Upon operation, the system was continuously outputting high-pressure values no matter the orientation of the control wheel. Troubleshooting this malfunction took several trials, as well as numerous prototypes. After several attempts at functionalizing the system, a high-pressure build up beneath the control wheel was discovered to be the cause of the continuous, high-pressure readouts. This was clear as the control wheel itself consistently rose out of its docking site within the main chip. While the fabrication process was simplified immensely and leakage was significantly reduced, we decided

the device needed an exhaust port to allow excess pressure to escape. This crucial modification need was taken into account for the subsequent iteration. The improved pressure leakage and resulting lack of pressure differential data can be seen in Figure 3.2.1.

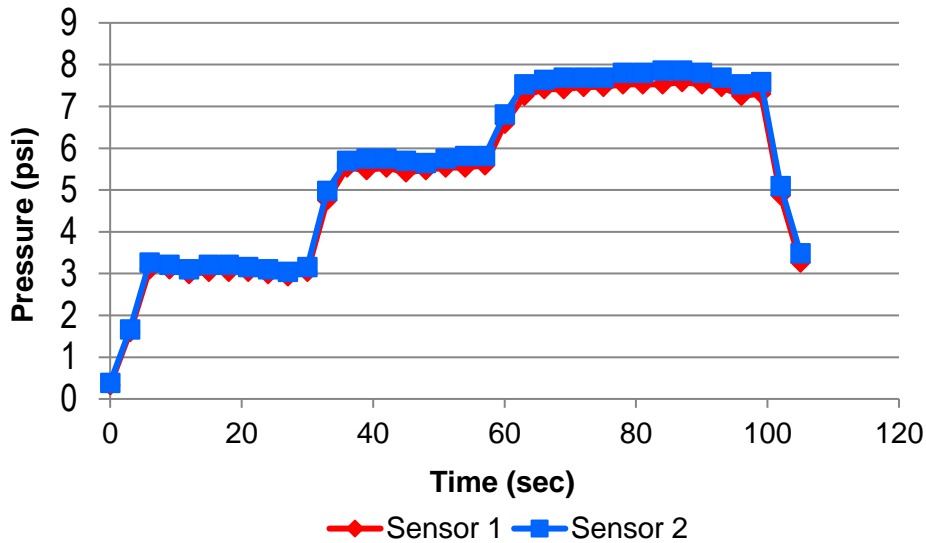


Figure 3.2.1: Pressure was applied at 5 psi, increased to 8 psi, and then finally to 10 psi before being disconnected entirely. The leakage is consistently a loss of about 2 psi, far better than our previous iteration. However, there is nearly no pressure differential even though sensor 1 was not connected to a channel in the outer array of the main chip and sensor 2 was connected to a channel in the outer array of the main chip.

3.3 3D Printed Mold Method W/ Pressure Exhaust

Throughout this iteration, several versions of the same conceptual design were tested. The most promising results came from a device with a small hole in the glass substrate bonded to the bottom of the device. The exhaust port allowed for the high-pressure pocket underneath the control wheel to escape from the bottom instead of being forced into the channels. The exhaust port was small, which caused the pressure to leak slowly, but after ample time, the differential was evident.

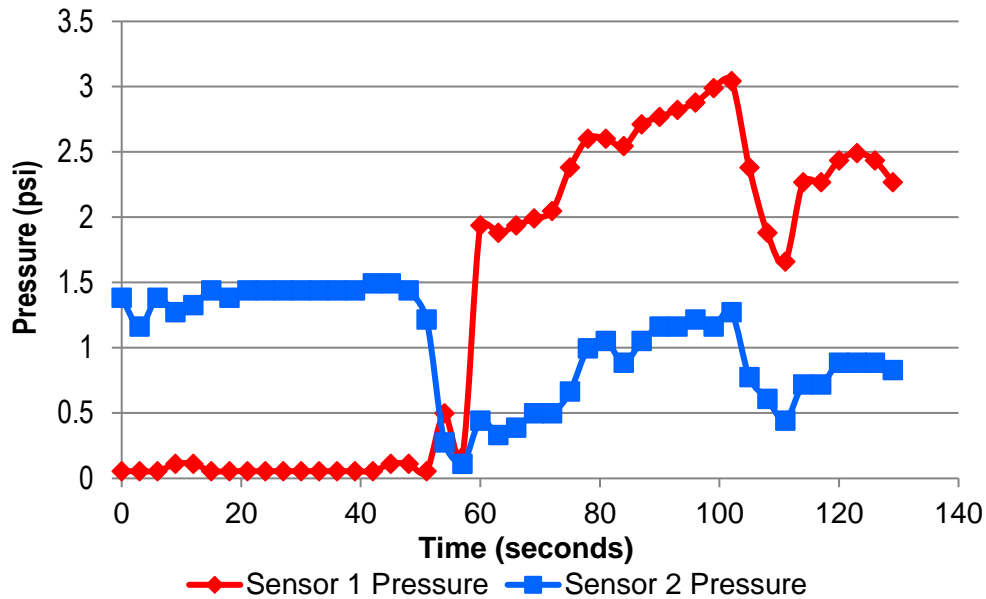


Figure 3.3.1 Two adjacent pressure sensors shown with their continuous pressure readings. Sensor 1 reads ~0 PSI when the channel is disconnected, while Sensor 2 has around 1.5 PSI at its output. Upon rotation, the sensors show the switch from a high to low state for Sensor 2, and vice versa for Sensor 1. Input pressure was 10 psi.

As shown in the figure above, it is clear that dynamic pressure differential and reduced cross talk are both achievable with single layer PDMS device. The variability in data after the sixty-second mark is due the user applying varying pressure in attempt to best align the channels under the microscope. One of the major drawbacks from this design is the high amount of leakage, and as a result the low amount of pressure that reach the desired channels. With the exhaust port in place, any pressure that is not entering directly into a channel is able to escape from the system. In order to reliably control a valve, there needs to be at least 5 PSI at the output of our device. Because of this lack of pressure when the channels are connected, modifications were made in the following iteration as to eliminate this issue.

3.4 Laser Cut Control Wheel Redesign

Excessive leakage through the exhaust port was the main issues in the previous design. The previous system used a PDMS control wheel with a thin layer of PDMS bonded to the bottom of the wheel to seal the channels from the exhaust port. In this iteration the

control wheel was laser cut in a heptagonal design and channels were rastered after. A chip was bonded to a glass slide, and a singular channel on the outer array was present to test for the accuracy and repeatability of the facilitated alignment. We rotated the device from one state, to another, and then back. We recorded a video in real-time of the dynamic testing and analyzed the step-wise images to determine if the facilitated alignment was sufficient for our needs. The heptagonal control wheel allowed for a smoother rotation and sufficiently aligned the inner and outer array.

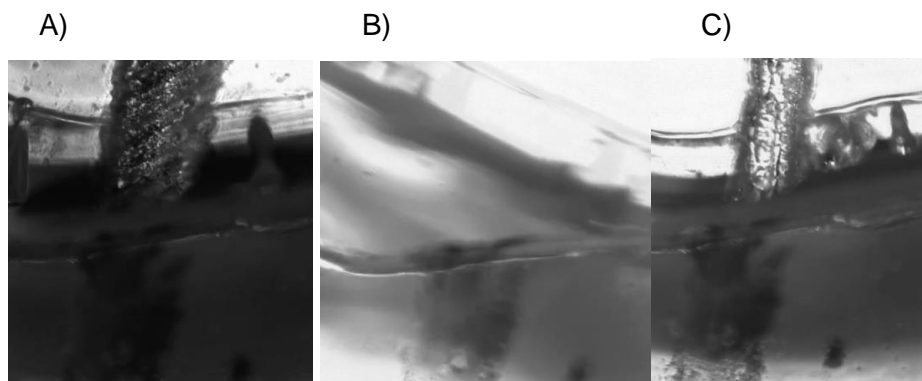


Figure 3.4.1 The three images above represent State 1, an interstate phase, and State 2. A) represents when channel 1 is connected to the target channel in the outer channel array. B) is showing the rotation phase when the heptagonal control wheel is facilitating the change and alignment of the second inner channel. C) represents the final state, where channel 2 is connected and properly aligned with the target channel. All of this can be done without the aid of a microscope because of the geometrical facilitation feature.

Testing will continue to see how the acrylic bottom seal will work with the entire system and preparation for a pressure test is currently taking place. Overall, this most recent iteration is our most appealing and easiest chip to operate, and a pressure test would further confirm its validity as a point of care device.

Chapter 4: Discussion

This project is on the cutting edge of microfluidics. Many research groups have attempted to provide a legitimate alternative to mLSI outside of a lab setting, yet none have achieved widespread success yet. In this section we will discuss what we have learned from the last year of research, and the significance of our findings.

4.1 Multilayer Method

The multilayer methodology was able to produce some of the most promising data. The fabrication of this device was extensive, and took several months to optimize the necessary number of layers. Both the PDMS ratios used in each layer, as well as the partial curing time had to be optimized using extensive trial and error. Eventually, testing of this iteration led to a collection of data that served as our initial proof-of-concept.

The sealing between layers, and between the interface of the control wheel and the main chip body were some of the biggest takeaways from this iteration. The multiple layer seal eliminated crosstalk as evident by the large pressure differential between connected and disconnected channels. It was necessary to assure that no pressure would be leaking between openings once supplied onto the chip. Any sort of leakage that occurred on chip would cause for unwanted valve actuation, rendering the technology severely flawed. Additionally, fabrication requirements were evaluated following the first phase of the project. After a careful evaluation, it was clear that fabrication of these devices needed to be simplified if they had any chance of future mass production. Since the goal of the technology was to reach rural, point-of-care clinics throughout the world, simplified fabrication was essential. Moving forward from this iteration, several key details were noted that needed to either be expanded upon, or needed to be changed in order to keep the system as robust as possible. Maintaining a cross-talk near zero, ensuring an adequate seal between the control wheel and the main chip body, and simplifying the fabrication of the device were all pieces of information that were streamlined into the design of the subsequent iteration.

4.2 3D Printed Mold Design

As 3D printing becomes exponentially more popular in the engineering world, the benefits it could have for microfluidic device fabrication are becoming more evident. There are now several 3D printers on the market that claim capabilities of printing features in the micron scale range necessary for microfluidic devices.

For this phase of the project, 3D renderings of microfluidic molds were produced using software such as SolidWorks and then sent to a third party printing operation, ShapeWays, to be printed for use. Upon receiving the molds, several initial PDMS chips were produced and analyzed. The surface roughness resulting from the 3D printed molds was evident to the naked eye, but it was unclear if this roughness would prove detrimental to the functionality of the device. Several devices were prepared and tested using our standard protocol. The majority of this phase of the project was riddled with data that was not in accord with the promising data from the previous iteration. Since the main focus of the new design was to simplify fabrication, the reduction of layers and use of 3D printed molds had clearly been at the expense of feature resolution.

There were several attempts made to solve this problem. The majority of effort was spent on a partially cured, bottom layer bonding technique where the main chip body and the central control wheel were placed onto a partially cured, spin-coated thin layer. The partially cured layer was still soft which would allow for the chip to sink into it and fill any imperfections resulting from surface roughness. This layer was optimized and the channels appeared much better after trial and error with the curing time and ratio of this thin bottom layer.

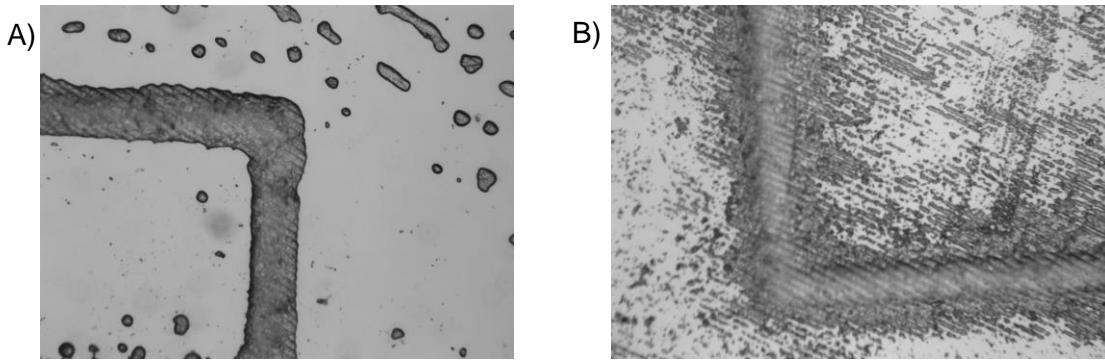


Figure 4.2.1: A) Chip made using 3D printed molds with thin layer and resulting improved surface roughness. Thin layer was spun at 1000 rpm for 60 seconds and cured 6.5 min at 80° C.
 B) Chip made using 3D printed molds without bottom thin layer and the resulting surface roughness.

Unfortunately, in the end it was discovered that due to the perfect uniformity of the control wheel to main chip interface, too much pressure was building up under the control wheel. The 3D printed molds had radii that were extremely close in size, which made for a perfect seal. However, because of this sealing, there was a strong buildup of pressure beneath the control wheel which was causing both the control wheel to be lifted out, as well as all of the channels to be reading high pressure at all times. Once the thin layer was optimized, it was clear this had to be the issue causing our unreliable results. Alterations were made to alleviate the pressure buildup issue, that further confirmed our suspicions about this issue.

4.3 3D Printed Mold Design with Pressure Exhaust

After going from a highly reliable, and repeatable pressure differential in the first iteration to no pressure differential at all in the second, some design changes were conceptualized to eliminate this issue. The resolution that provided the most realistic, but also thorough solution to the problem, was incorporating a pressure exhaust into the bottom of the rigid substrate that the microfluidic chip sits on. This pressure exhaust would allow for any unwanted pressure to be released through the bottom of the device, while leaving the desired pressure inputs uninterrupted. Alleviating the pressure beneath the central control wheel is an essential change, and this design had the potential to do so.

To properly address an exhaust port, there needed to be a consistent way of producing substrates with a consistent diameter of exhaust, as to standardize the rate of leakage through the bottom of the device. The initial exhaust port was created by puncturing a glass microscope slide, giving the device a small slit for superfluous pressure to escape. Although the production of this substrate with a hole was successful, it is very difficult to recreate as the glass slides are too ductile to accurately remove a circular region without cracking them. It was evident that an alternate material, and method of producing the exhaust port was necessary. To do this, an Epilog Laser Cutter was used to produce several rigid substrates, composed of acrylic, that could be reusable. Experiments are being done to continue optimizing these acrylic substrates, as to provide the most efficient exhaust port dimensions.

4.4: Laser Cut Control Wheel Redesign

Using all the information learned from our previous iterations, as well as their sub iterations not explicitly discussed, our team is in the midst of a complete redesign. We have learned that to accomplish all of our goals, we need to create a device that will be able to do all of the following:

- Maintain strong enough pressure to close valves
- Reduce crosstalk to the point that will leave desired valves open
- Minimize leakage -- both between channels, and throughout chip
- Tight fit and easy rotation of control wheel to main chip
- Ability to open and close valves without the aid of a microscope
- Strong bonds between layers

These considerations have led us to our most recent, and by far most practical design for POC applications. This design has yet to undergo pressure testing, but it has the potential to meet all of the requirements above. Most importantly it can be operated without the aid of a microscope, a feature none of our previous iterations could

accomplish. We have accomplished all of the requirements in at least one of the previous iterations, so the geometrical facilitated design is very significant.

4.5 Engineering Standards and Realistic Constraints

During the course of this project, our team had to consider various social justice standards.

4.5.1 Economic

Our device design has economic implications because of the simplicity of its operation, as well as the ease of its fabrication. One of the key goals of the project was to reduce the amount of peripheral equipment required to successfully operate these microfluidic systems, if not completely remove it. The biggest drawback of the equipment required to operate mLSI experimentation is that the multiple components are all very expensive. This expense limits the number of potential users because of budgeting issues. After eliminating this aspect of the testing setup, the overall price of the device is reduced significantly. A chart has been included below, denoting each component of our novel microfluidic system, and its' relative price.

Table 4.5.1.1: Economic Considerations

Item	Cost per Unit (Dollars)
Acrylic Sheet	\$0.47
Pneumatic Tubing	\$0.33
PDMS	~\$150/ (Kg) ³
Aluminum Down Tube	\$0.05

4.5.2 Health and Safety

Since PDMS, acrylic, and the other, much smaller components of our device are all non-toxic, the use of our device by a scientist is entirely safe. The production of the

device itself has some chemicals that are vital to the process but also have slight health risk implications. A list of dangerous chemicals used during fabrication can be found below.

Table 4.5.2.1: Health and Safety Considerations

Item	Danger Level
TMCS (Trichloromethylsilane)	High (Inhalation, Ingestion, Skin contact)
HDMS (Hexamethyldisilazane)	High (Inhalation, Ingestion, Skin contact)
Acetone	Low (Inhalation, Ingestion, Skin Contact)

4.5.3 Sustainability

We are seeking to create a robust, highly functional device that can allow for the use of mLSI technologies in rural, POC clinics. One of the most important requirements for this to be possible is to reduce waste as much as possible. Because our target market resides in rural locations, most often in third-world countries, having to constantly bring in more equipment for experimentation is not an option. With this in mind, we decided to tackle these challenges with a reusable microfluidic system that would contain a flushing capability to allow for several trials of experimentation before the device is no longer efficacious.

4.5.4 Social

The need for easy-to-use, robust microfluidic systems in rural, POC clinics is becoming more and more evident to the scientific community. The reduction in cost and sample volume makes for benefits that affect clinicians and patients. Our system looks to bridge the gap between cutting-edge scientific breakthroughs and the people who need them the most but cannot access them without some degree of price-point reduction. Cheap, simple microfluidic platforms are the future of POC clinics, and we are striving to be at the forefront of this movement.

4.5.5 Ethical

It is vitally important when bringing a novel system to the public that the claims being made from the R&D phase are indeed true. The complete optimization of these devices is essential before it can be used for human testing. Our team is committed to transparent, honest science, making sure that every claim being made is true and can be backed by reliable data.

Chapter 5: Future Work and Conclusion

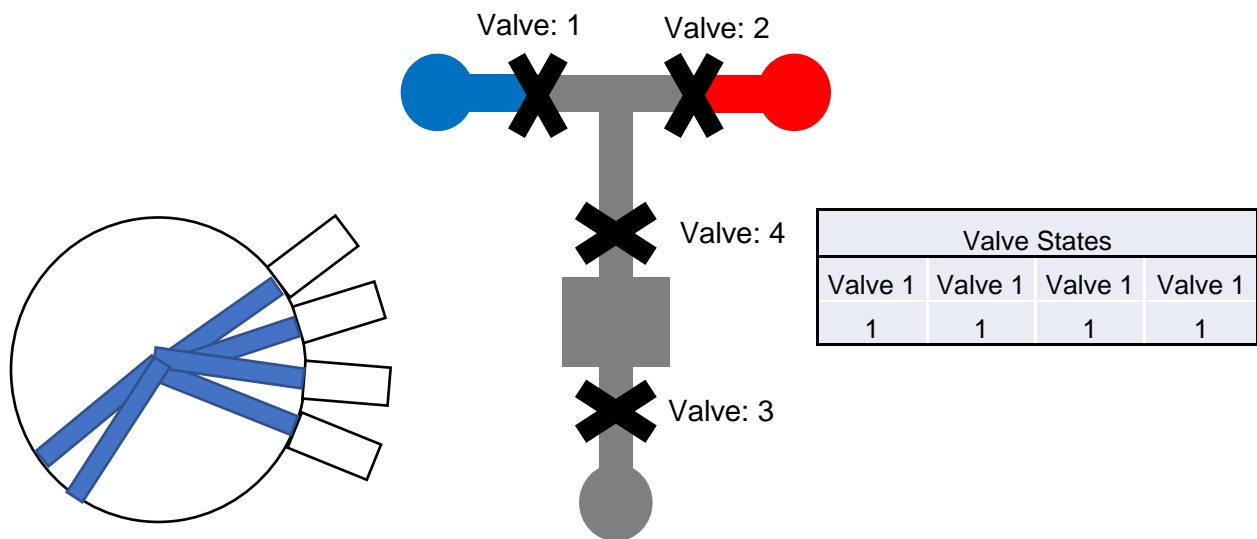
5.1 Future Studies

Our most recent findings proved we can facilitate changes in valve actuation without the use of a microscope. We are going to focus our next efforts on creating a fully functional device that uses the geometric-assisted alignment system. Following initial tests with this system, we have concluded that the heptagonal, laser-cut control wheel works the best. Our next step is finding an appropriate way to enclose our laser cut channels. Currently they are not enclosed. The difficulty will be finding a bonding method that does not damage the integrity of the channels. We must also find a thin rigid material for this bottom piece of the control wheel. This layer needs to be relatively thin to allow for proper vertical alignment of our inner to outer channels. The main chip body is made of PDMS, and PDMS doesn't bond well to plastics. So the PDMS and control wheel cannot be bonded to the same piece of material.

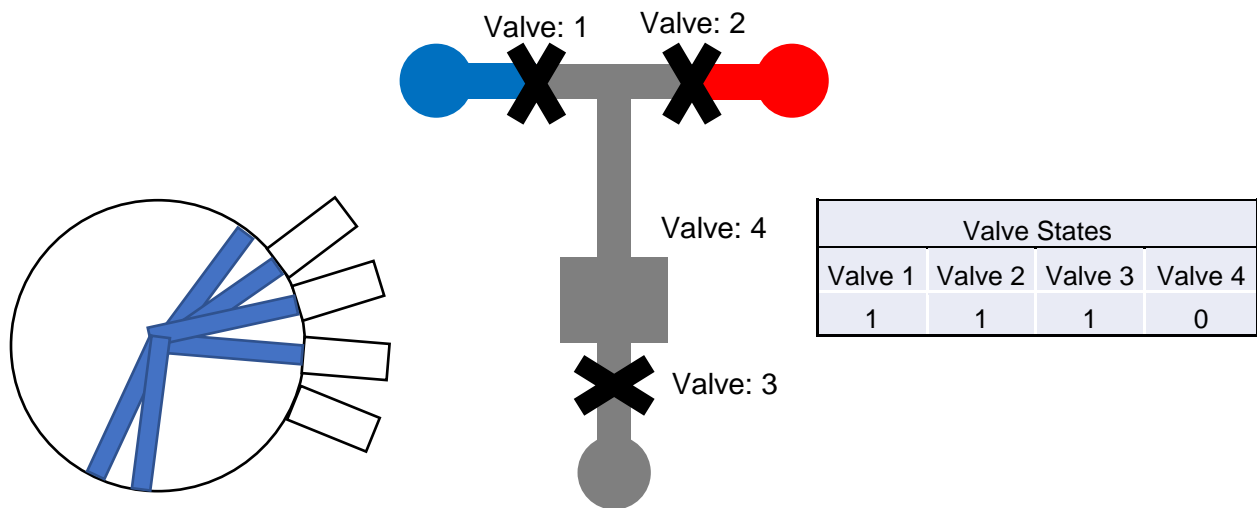
We are also exploring a portable pressure source. Our current source is a 6-gallon air compressor. While this sort of compressor could easily exist in POC clinics, it would be very beneficial if our system could have a portable pressure source accompanying our microfluidic device. We are currently researching what type of pressure sources are available on small scale and analyzing them based on cost and functionality.

The proof of concept test we need to demonstrate our device is ready to directly aid diagnostic capabilities in at the point of care is the fluidic mixing test. We hope to mix red and blue food dyes in our on chip diffusion chamber. We have had this goal in mind for a while but have focused on optimizing the crosstalk and material composition of our device. By rotating through a specific sequence of valve combinations, we hope to achieve successful mixing that is visually illustrated below in our flow chart bitmap in Figure 5.1.1.

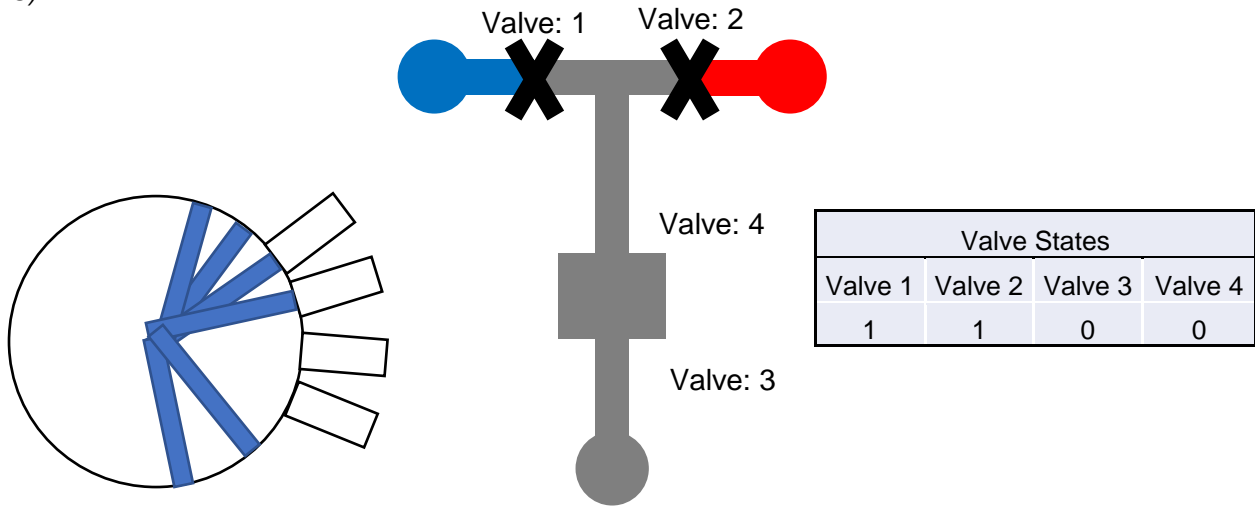
A)



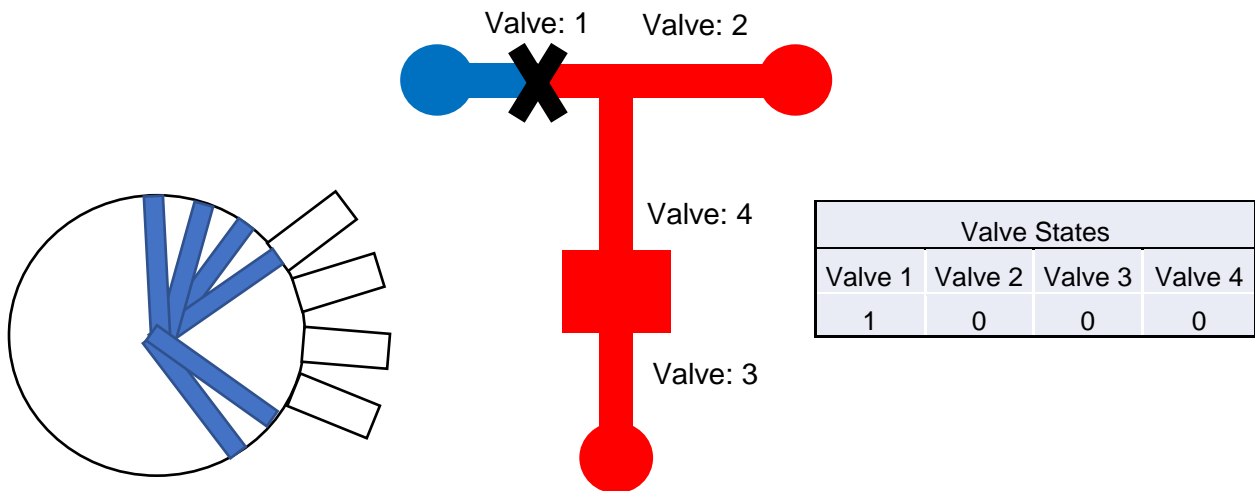
B)



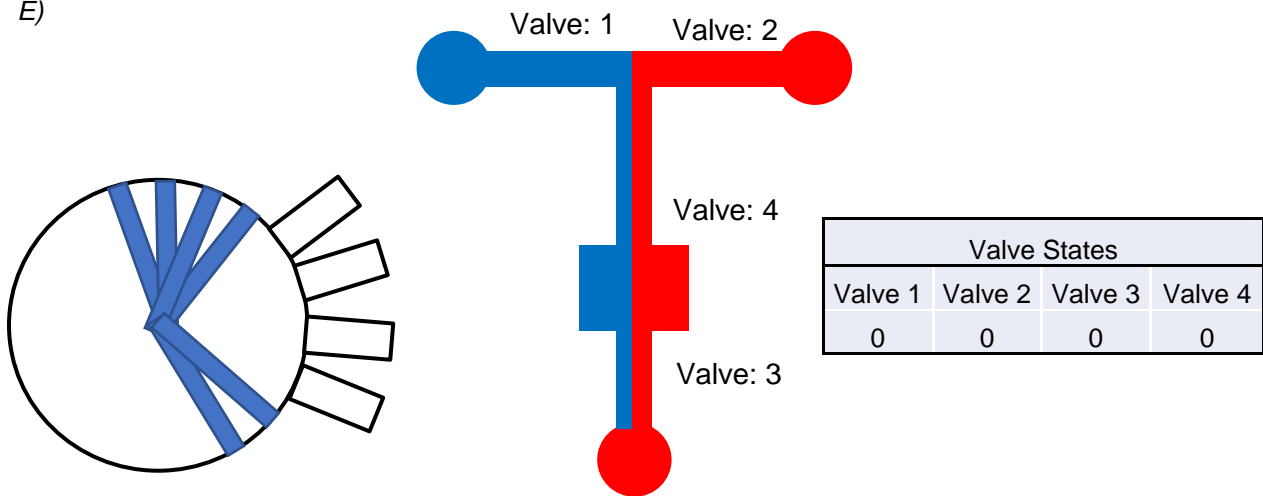
C)



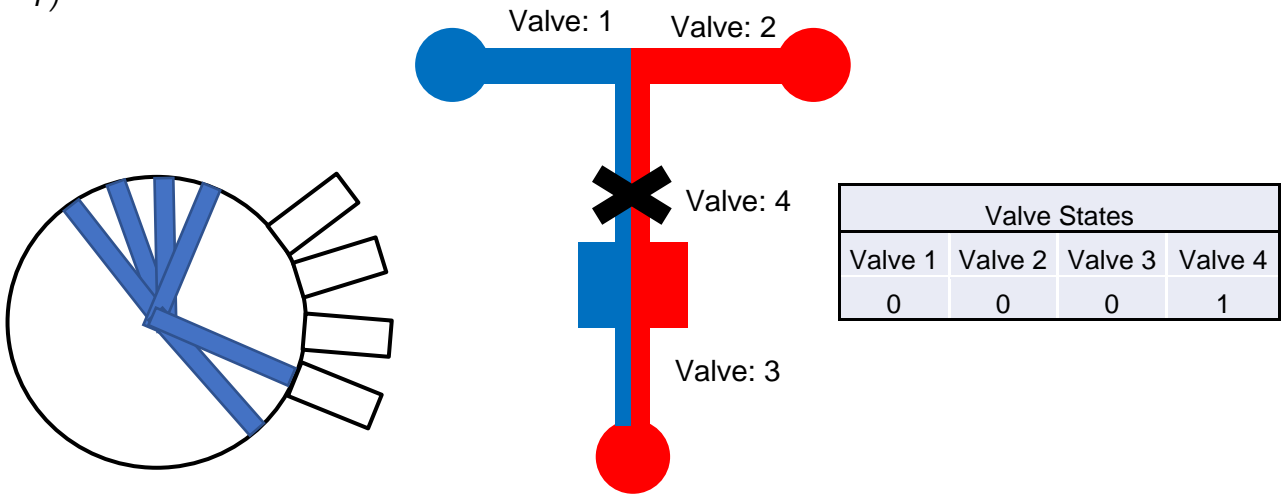
D)



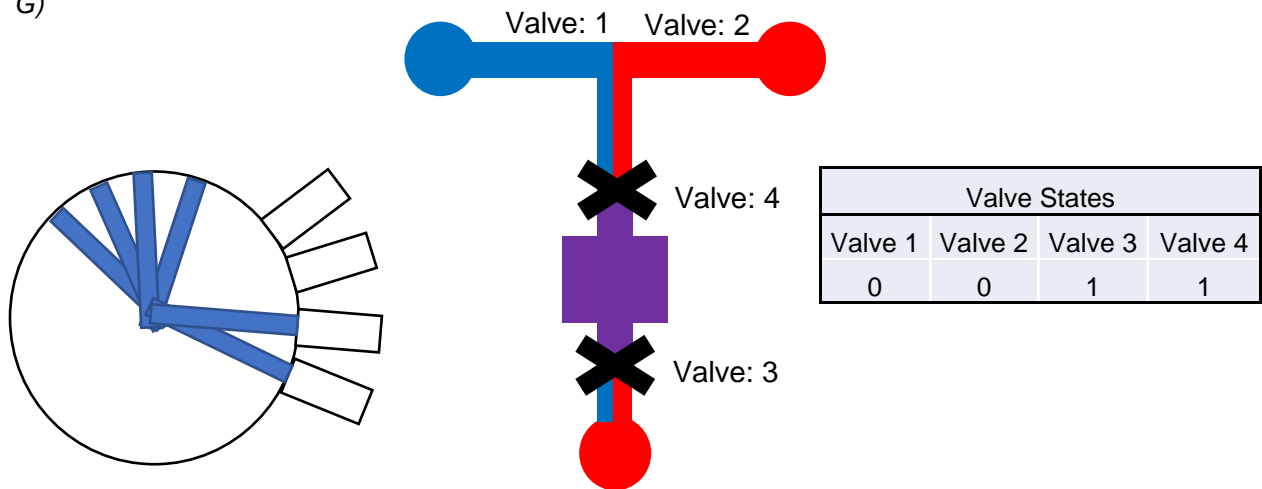
E)



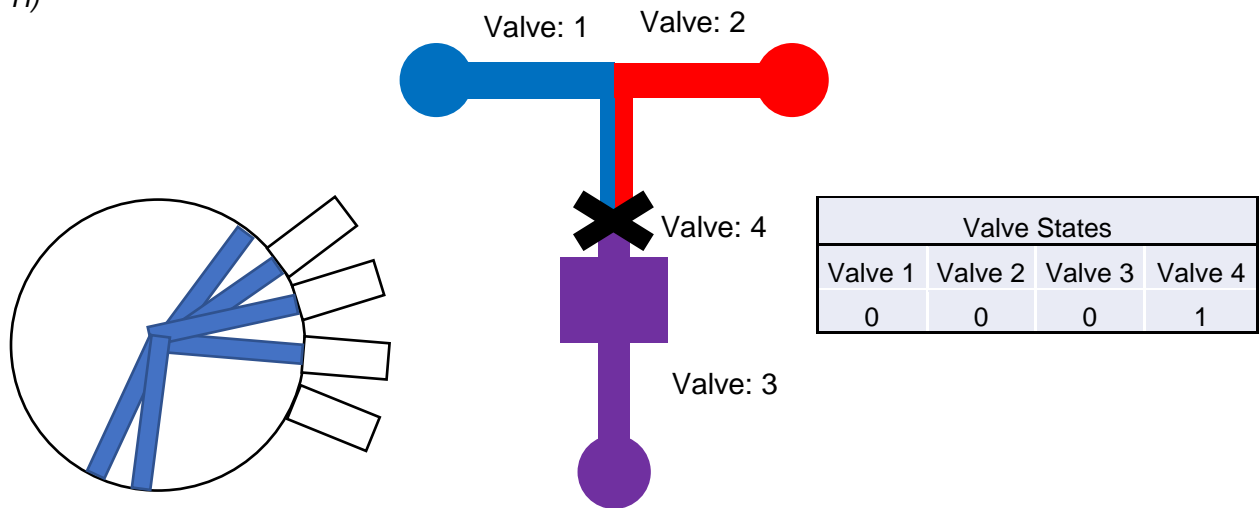
F)



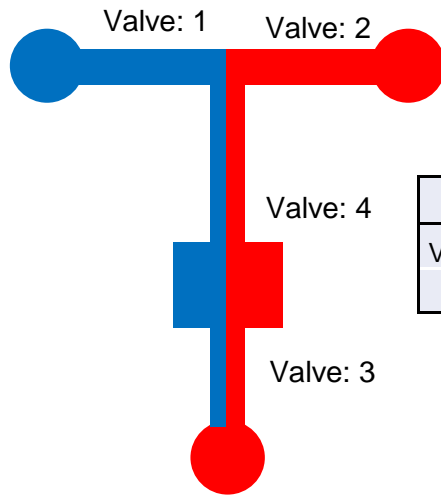
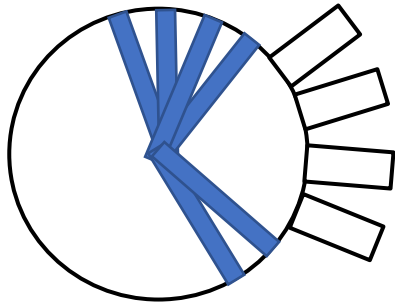
G)



H)

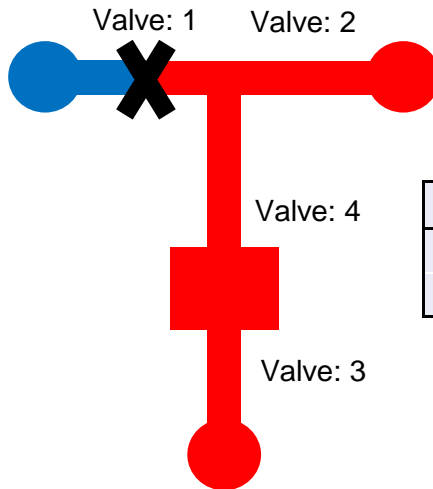
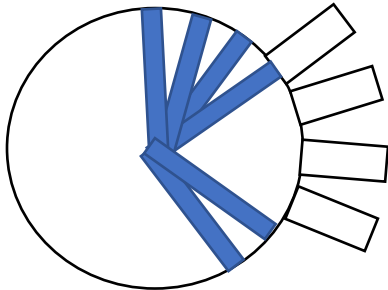


I)



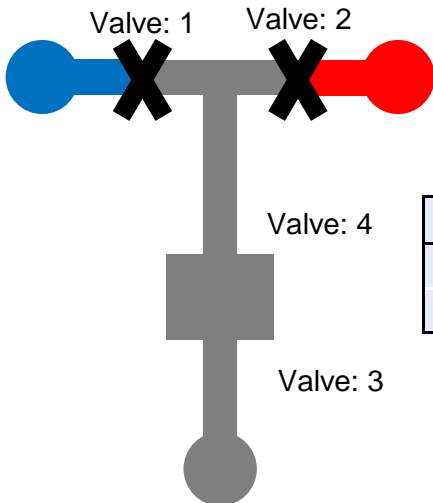
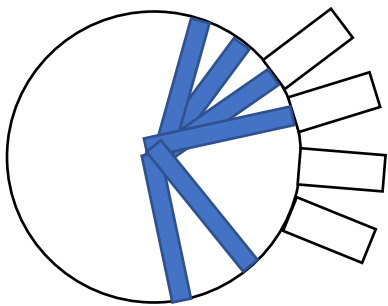
Valve States			
Valve 1	Valve 2	Valve 3	Valve 4
0	0	0	0

J)



Valve States			
Valve 1	Valve 1	Valve 1	Valve 1
1	1	1	1

K)



Valve States			
Valve 1	Valve 2	Valve 3	Valve 4
1	1	0	0

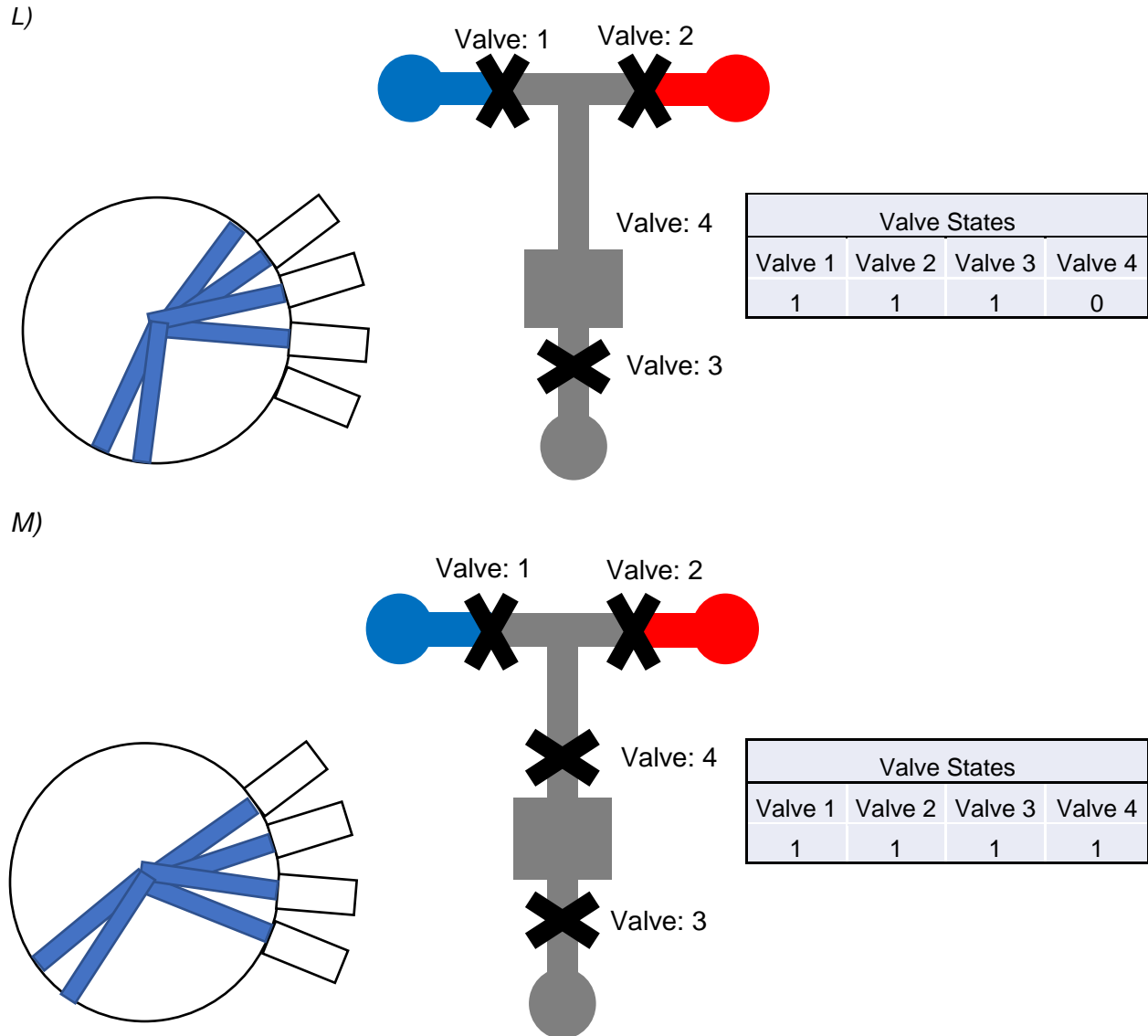


Figure 5.1.1: Flowchart Bitmap. The circular wheel on the left of the images represents the control wheel and its inner connections to the outer array of the main chip body. The valve state tables indicate whether the valve is pressurized (1) or depressurized (0). The t-shaped illustration is a visual illustration of our flow layer and the desired resulting visual confirmation of red and blue food dye mixing.

5.2 Future Applications

Rural clinics throughout the world make use of simple testing platforms to aid in the diagnosis of disease that are common to those areas. Robust systems that can allow for high degree of detection of these disease states are in very high demand. HIV and

malaria are some of the most common disease states that these rural clinics seek to diagnose. Both of these conditions are very serious and can lead to an extremely high number of deaths if not detected early. Since these two disease states are so common across third world countries, numerous detection methods have been developed. Along with these detection techniques, portable systems have been optimized so that they can be efficiently transported and used by the clinicians. ELISA, or enzyme-linked immunosorbent assays, is one of the most commonly used detection techniques. Our team seeks to develop the microfluidic control system at hand into an ELISA platform that can aid in the early detection of HIV. Since highly efficacious testing methods have already been developed for the detection of this disease all that must be done is scaling them to our microfluidic device. There are future plans, once the control aspect of our system has been optimized, to fully develop the device into a microbiological assay system that makes use of ELISA to test for the presence of HIV in human samples.

5.3 Closing Remarks

In total, we have developed a dynamic, robust, and scalable microfluidic control system that can allow for this innovative technology to reach parts of the world that it never would have before. Our portable system allows for minimally trained clinicians and scientists to reap the rewards of mLSI technologies by simplifying previously complex operation protocol into a user-friendly, single-step system. This innovative technology has the potential, when fully optimized, to penetrate the rural clinic market and make a difference for those in need, worldwide.

References

Begolo, Stefano. "Instrument Free Control of Microfluidics." *ALine, Inc. - Accelerated Microfluidic Development*. MicroTAS, 11 Oct. 2016.

Du, Wenbin., et al. "SlipChip." *Lab on a Chip*. The Royal Society of Chemistry, 15 May 2009

Esquivel, Juan Pablo, et al. "Fuel Cell-powered Microfluidic Platform for Lab-on-a-chip Applications." *Lab on a Chip*. The Royal Society of Chemistry, 10 Nov. 2011.

Gómez-Sjöberg, Rafael., et al. "Versatile, Fully Automated, Microfluidic Cell Culture System." *ACS Publications*. American Chemical Society, 23 Oct. 2007.

Harper, Jason C., et al. "Magnetic-adhesive Based Valves for Microfluidic Devices Used in Low-resource Settings." *Lab on a Chip*. The Royal Society of Chemistry, 28 Sept. 2016.

Perry et al.. "Design Rules For Pumping And Metering Of Highly Viscous Fluids In Microfluidics." *LoC* 2010.

Wang, YJ, et al. "An Integrated Microfluidic Device For Large-Scale In Situ Click Chemistry Screening." *Lab On A Chip*. 16 Sept. 2009.

Wentao, Li., et al. "Squeeze-chip: A Finger-controlled Microfluidic Flow Network Device and Its Application to Biochemical Assays." *Lab on a Chip*. 23 Feb. 2012.

Appendices



```
voltage_arduino_code | Arduino 1.6.9
File Edit Sketch Tools Help

voltage_arduino_code

int timer = 3000;

void setup() {
  // put your setup code here, to run once:
  Serial.begin(9600);
}

void loop() {
  // put your main code here, to run repeatedly:
  //read input on pin A0
  int sensorValue = analogRead(A0);
  int sensorValueb = analogRead(A1);
  //convert analog reading to voltage
  float voltage = sensorValue * (5.0 / 1023.0);
  float voltageb = sensorValueb * (5.0 / 1023.0);
  //print out value
  Serial.println(voltage);
  Serial.println(voltage);
  Serial.println(voltageb);
  delay (timer);
}
```

Figure A.1: Arduino code. We wrote this code to take voltage measurements of two pressure sensors every 3 seconds. The time between measurements was often varied depending on the experiment.

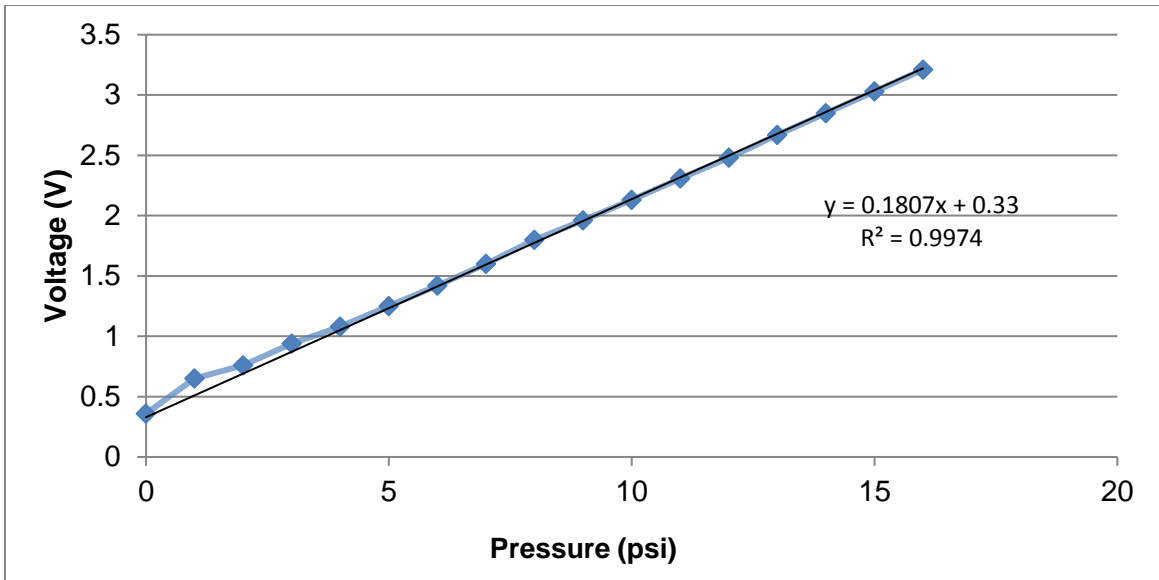


Figure A.2: Pressure vs. Voltage data. This data was taken via our Arduino code and used to develop a relationship of input pressure to our pressure sensors, and their resulting output voltage. This relationship was used to convert all subsequent voltage readings from our pressure sensors into pressure readings.